



Effect of ionic strength and calcium ions on humic acid fouling of hollow-fiber ultrafiltration membrane

Yongwang Liu^a, Xing Li^{a,*}, Yanling Yang^a, Wanlu Ye^b, Jiawei Ren^a, Zhiwei Zhou^a

^aKey Laboratory of Beijing for Water Quality Science and Water Environment Recovery Engineering, Beijing University of Technology, Beijing 100124, China, Tel. +86 10 67391726; email: lixing@vip.163.com

^bBeijing City Planning Technical Service Center, Beijing 100045, China

Received 10 October 2013; Accepted 13 March 2014

ABSTRACT

Effect of ionic strength and calcium ions addition on the molecular properties of humic acid (HA), as well as the HA rejection coefficient and fouling characteristics of ultrafiltration were investigated in this study. Experiments were performed with an immersed hollow-fiber polyvinyl chloride membrane at a laboratory scale. The results indicated that both ionic strength and calcium ions could effectively reduce zeta potential of the HA solution. Average size of HA was identical with various ionic strength (10, 20, and 40 mM) or low calcium ion concentration (0.5 mM), but a much larger HA size was obtained with higher calcium ion concentrations (1.0 mM or 2.0 mM) for the complexation interaction between HA molecules. The ionic strength significantly reduced the HA removal, and somewhat mitigated the membrane fouling for the reduction of electrostatic repulsive forces between HA molecules and the membrane surface. At a low calcium ion concentration, the surface complexation dominated the fouling behavior of the process, and led to an increase of cake fouling resistance. However, at higher calcium ion concentrations, the bulk complexation dominated the interaction fouling behavior of the process, leading to a reduction of both cake fouling and pore blocking for the larger size aggregations.

Keywords: Humic acid; Calcium ions; Ionic strength; Ultrafiltration; Membrane fouling

1. Introduction

Ultrafiltration (UF), a low-pressure membrane filtration process, has been widely applied during the past decades in drinking water treatment for the removal of particles, turbidity, micro-organisms, and pathogens from surface water and groundwater [1]. The application of UF in drinking water treatment is considerably constrained by membrane fouling caused

by the accumulation of contaminants on the surface or within the pores of the membrane over time. Membrane fouling contributes to increased operational costs associated with higher trans-membrane pressure (TMP) and the need for frequent chemical cleaning as well as shortened membrane service life [2]. Recent studies have shown that humic acid (HA), as the main component of natural organic matter, is a major foulant during UF of surface water [3–5]. A large number of studies have conducted to identify the fouling characteristic of HA, as well as synergy effects with particles or other organic matter [6–9].

*Corresponding author.

Previous studies indicated that membrane fouling of HA was affected by many factors, including the characteristic of the HA molecule and membrane surface, operating conditions, and solution environment of the feed. The solution chemistry, such as calcium ion and ionic strength concentration, may affect the conformation and electrostatic repulsive force of the molecules, and therefore has a significant impact on the interaction between foulants and the membrane surface. Yuan et al. [5] found that the flux at the end of the two-hour filtration varied from 5.2×10^{-5} m/s in deionized (DI) water to 2.6×10^{-5} m/s in the presence of 100 mM ionic strength, and 1.0 mM calcium ions also caused a significant increase in the rate of flux decline, which was well agreeable with the findings of Shao et al. [10]. However, Qu et al. [11] reported that the flux decline was apparently improved with 2.0, 5.0, and 10.0 mM calcium ions addition for the improved adhesion on the membrane surface. Moreover, Tian et al. [12] observed that ionic strength could mitigate the membrane fouling of HA. Therefore, further studies are required to investigate the effect of different cations on HA fouling of UF membrane to elucidate the above-mentioned divergence.

The aim of this study was to investigate the effect of ionic strength and calcium ions on HA properties, as well as the membrane fouling characteristics in the hollow fiber UF process. Experiments were performed with an immersed hollow-fiber polyvinyl chloride (PVC) membrane at a laboratory scale, the membrane has been extensively used for drinking water treatment with more than 485,000 m³/d in China to this point. Fouling resistance distribution, including cake fouling and pore blocking, were performed to access the contribution of ionic strength and calcium ions on fouling resistance.

2. Materials and methods

2.1. Experimental materials

HA (Jinke, China) was used as the model foulant in this study. HA (5 g) was dispersed in 0.1 mM NaOH, and mixed for 24 h by a magnetic stirrer. The suspension was filtered by a 0.45 μm cellulose acetate membrane (Taoyuan, China) to remove the undissolved part, afterwards, the pH of the filtered solution was adjusted to 7.5 using 0.1 mM NaOH (Beijing Chemical, China) or HCl (Beijing Chemical, China). Then, the solution was diluted to a volume of 1,000 mL and stored in the dark at 4°C. The HA solution was diluted to 20 mg/L with DI water, solution pH was adjusted to the desired value using small amounts of HCl or NaOH. NaCl of 0.1 M (Fuchen,

China) and 0.1 M CaCl₂ (Fuchen, China) were used to prepare the background electrolyte solution. All chemicals used in this study were analytically pure.

The apparent molecular weight (MW) distribution of the HA sample was determined using the UF fractionation method. HA samples were fractionated in a 76 mm diameter stirred cell (Amicon 8400, Millipore, USA) using a series of regenerated cellulose UF membranes (Millipore Corp., USA) with nominal MW cut-offs of 1, 3, 10, 30, and 100 kDa. The filtration was performed at a constant pressure of 100 kPa, with the fractional amount of HA within each size range calculated from the difference in HA concentration between adjacent filtrate samples.

A hollow-fiber UF membrane module (Litree, China) with a total surface area of 0.017 m², which is made of PVC, with a nominal pore size of 0.01 μm, an internal diameter of 0.8 mm, an outer diameter of 1.45 mm, and a length of 25 cm, was used in this study. The new membrane was immersed in DI water for at least 24 h before using to remove any residual storage agent.

2.2. Experimental methods

A schematic illustration of UF experiment is shown in Fig. 1. The raw water was fed into a constant-level tank to manipulate the water head for the subsequent unit. The membrane module was submerged in the cylinder, and continuous aeration was provided at the bottom of the cylinder to wipe the membrane. The effluent was collected directly from the membrane module by a peristaltic pump. A manometer, connecting with a programmable logic controller, was installed between the membrane module and the peristaltic pump to monitor the TMP periodically. The UF process was conducted with a dead-end filtration mode at constant flux of 50 L/(m² h), corresponding to a hydraulic retention time of 0.5 h. Permeate samples were collected periodically for subsequent concentration analysis.

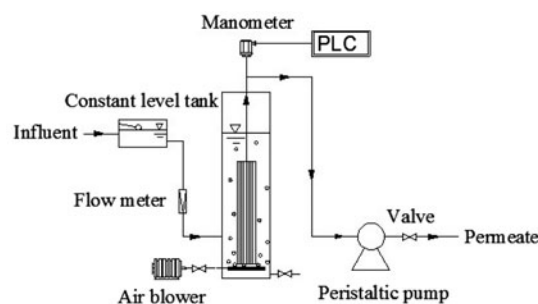


Fig. 1. Schematic diagram of UF system.

2.3. Fouling analysis

The resistance-in-series model proposed by Choo and Lee [13] was used to analyze the fouling resistance distribution. The filtration of ultrapure water with new membrane was conducted to calculate R_m . At the end of every filtration experiment, the HA solution in the cylinder was discharged, then refilled with ultrapure water for estimating R_t , afterwards, the membrane was cleaned with cotton gently to remove the cake layer on the membrane surface in order to evaluate the $R_m + R_p$.

$$R_t = R_m + R_c + R_p \quad (1)$$

$$R_m = \frac{P_0}{\mu J} \quad (2)$$

$$R_c = \frac{P_t - P_c}{\mu J} \quad (3)$$

$$R_p = \frac{P_c - P_0}{\mu J} \quad (4)$$

where μ was fluid viscosity (Pa s), J was the permeate flux (m/s), R_m was the intrinsic membrane resistance (m^{-1}), R_c was the cake fouling resistance (m^{-1}), R_p was the pore blocking resistance (m^{-1}), and P_0 was the TMP of the new membrane (Pa), P_c was the TMP after physical cleaning (Pa), and P_t was the TMP at the final filtration (Pa).

2.4. Analysis methods

HA concentration of the permeate and at the inlet were evaluated by a UV/Vis spectrophotometer (T6, Puxi, China) with the absorbance measured at 254 nm. zeta potentials of the samples were measured with a zeta potential analyzer (Nano-Z, Malvern, England). The size distribution, sized between 0.6 nm and 7 μ m, was measured with DelsaNano S (Beckman Coulter, USA) at 25°C, which was based on dynamic light

scattering (DSL) analysis. pH value was determined and calibrated daily using pH buffer solutions. The temperature was measured with a alcohol thermometer.

A piece of membrane was cut from the membrane module, and flushed with DI water gently to remove the unfirmed foulants. It should be dried 24 h in a dryer at room temperature before observing in the scanning electron microscope (S-4300, HITACHI, Japan), which was performed at coarse vacuum with an accelerating voltage of 15 kV.

3. Result and discussion

3.1. Zeta potential and size distribution of HA with ionic strength and calcium ions addition

Zeta potential, an indicator of the electric property, was used to investigate the effect of ionic strength and calcium ions on HA molecule. HA shows a negative charge in the pure water solution as it is made of carboxyl groups, phenolic groups, and other negative charge groups [14]. As shown in Table 1, zeta potential of HA changed from -43.9 to -23.7 mV with an ionic strength increase from 0 to 40 mM in the absence of calcium ions. With the addition of ionic strength, negative charged functional groups of the HA were shielded due to the double layer compression and reduction of charge at stern layer [3,15,16]. A same zeta potential change was achieved with the addition of calcium ions, which varied from -31.5 to -20.3 mV as the calcium ions increased from 0 to 2.0 mM with the ionic strength of 10 mM. It should be noted that calcium ions can increase HA aggregation by canceling the negative charge functional groups or by bridging the membrane surface with negative charge functional groups of HA [8].

Size distribution of HA with ionic strength and calcium ions addition was also conducted, the results were shown in Fig. 2. The main peak of HA was about 150 nm in pure water solution, and there was no change with gradual addition of ionic strength, then, it can be concluded that ionic strength had

Table 1
Effect of ionic strength and calcium ion concentrations on zeta potential of HA solution

	Calcium ions ^a (mM)				Ionic strength (mM)			
	0	0.5	1.0	2.0	0	10	20	40
Average zeta potential (mv)	-31.5	-28.6	-24.5	-20.3	-43.9	-35.13	-30.53	-23.7
Standard deviation (mv)	1.47	1.19	0.72	0.46	3.0	2.55	2.67	2.11

^aDetermined using 20 mgL⁻¹ HA solution with ionic strength 10 mM at pH 7.0, 25°C.

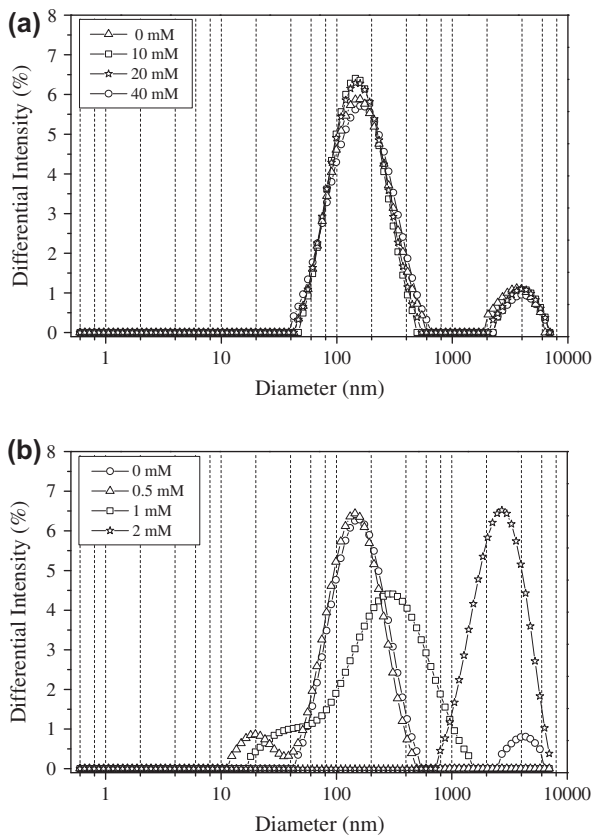


Fig. 2. Size distribution of HA at different ionic strength (a) and calcium ion (b) concentrations.

negligible influence on HA particle size. However, a study carried out by Zularisam et al. [8] revealed that the HA became more compact because their functional groups were shielded and the electrostatic repulsion was reduced. Here the change of HA size distribution was not observed with different ionic strength concentrations, or if present, the compaction was too small to be measured by DSL analysis. Interestingly, as compared to ionic strength, different changes were observed with relatively lower (0.5 mM) and higher (1.0 and 2.0 mM) calcium ion concentrations. On one hand, the size distribution of HA with 0.5 mM calcium ions was identical with the base case where no calcium ions was added. Calcium ions were usually thought to bind the carboxylic group of HA and leading to conformational changes. However, at low calcium ion concentration, the effective concentration of HA were similar, and aggregations between HA molecules did not occurred for the strong electrostatic repulsive force. On the other hand, in the case of higher (1.0 and 2.0 mM) calcium ion concentrations, the main peak of HA shifted to a larger scale compared to the base case, and a bigger particle size was

obtained with the higher concentration. This indicated that 1.0 or 2.0 mM calcium ions were enough to promote aggregations among HA molecules. The calcium ions preferentially bind to carboxylic groups of HA and form bridges among HA molecules, which can be explained by the so-called “egg-box” model [17]. Size distribution of HA plays a vital role in the rate and extent of HA rejection and membrane fouling, which will be discussed hereinafter.

3.2. Effect of ionic strength on HA removal, TMP, and fouling resistance distribution

The effect of ionic strength on HA removal and membrane fouling during constant flux UF were investigated, as shown in Fig. 3. It was observed that the HA removal at the beginning of the filtration was much higher than that of the following process, which was reasonable owing to rapid adsorption of HA into

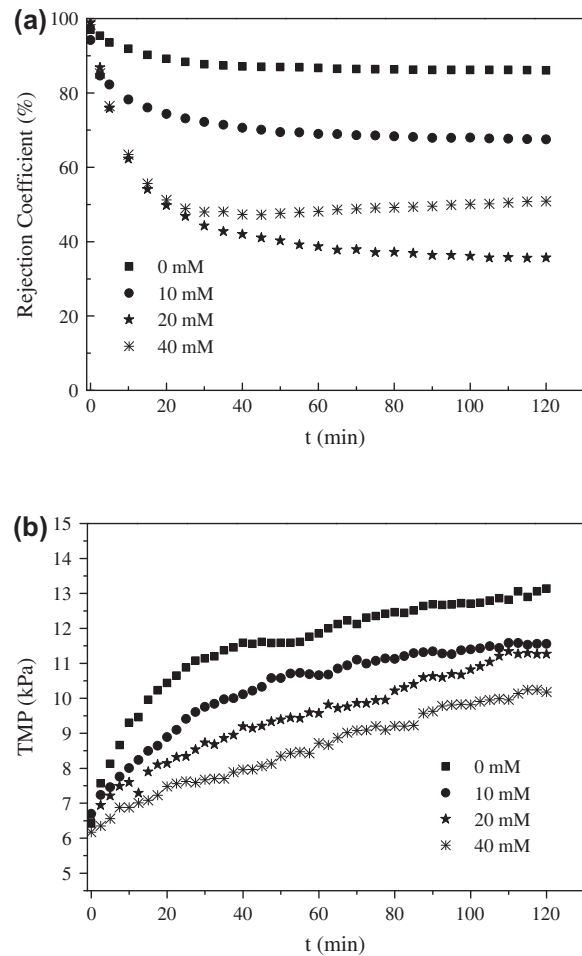


Fig. 3. Effect of different ionic strengths on HA removal (a) and TMP (b) development of the UF process.

the membrane pores and the surface [8]. The HA removal coefficient of the HA solution without any additive at the final filtration was about 86.1%; however, the percentage of HA components with MW greater than 100 kDa (the MWCO of the membrane in this experiment) was 73.4%, as plotted in Fig. 4. This phenomenon was mostly owing to the pore blocking that restricted membrane pores, and the compact cake layer formed on the membrane surface that rejected more HA molecules [18].

As seen from Fig. 3, ionic strength had a great influence on the HA rejection coefficient. At the end of the UF process, the HA rejection was 67.5% for the solution with 10 mM ionic strength addition compared to 50.9% for the solution with 40 mM ionic strength. There was a smaller value of 35.6% for the solution with 20 mM and much larger value of 86.0% for the solution without extra ionic strength added. A dramatic reduction of electrostatic repulsive forces between HA molecules and membrane surface would be achieved with the addition of ionic strength for reducing zeta potential of HA. Although the size distribution of HA was not affected by ionic strength, the decrease in electrostatic charge repulsion on the membrane surface allowed HA pass through the membrane easily, indicating that electrostatic interaction plays a more important role than pore size exclusion mechanism under the conditions tested [8]. Interestingly, HA removal rate was lower for ionic strength of 40 mM than that of 20 mM, and it was deduced that high ionic strength could cause considerable compaction of membrane pores, encouraging further restriction of HA [19].

As shown in Fig. 3, the ionic strength could mitigate membrane fouling; the increase of TMP was declined from 6.72 kPa without ionic strength to 4.93,

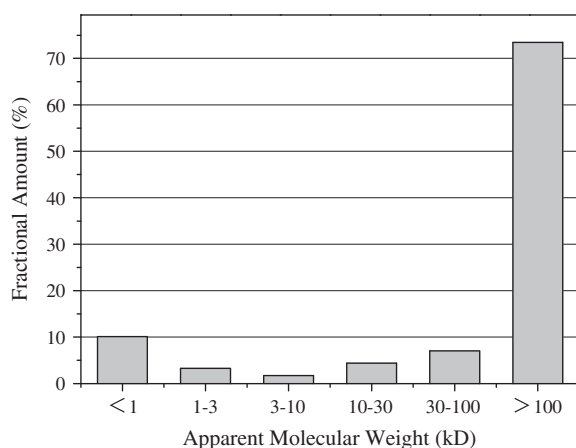


Fig. 4. Apparent MW distribution of HA at pH 7.0.

4.60, and 4.01 kPa with 10, 20, and 40 mM, respectively. The ionic strength was able to decrease the stretching degree of HA molecular structure by neutralizing its negative charges, thus decreasing electrostatic interaction between HA and membrane surface. In such case, it was easier for HA molecular to pass through membrane pores. This result was consistent with Tian et al. [12] who observed that ionic strength addition reduced the total fouling resistance of HA.

To further observe how ionic strength affects various fouling resistances, we conducted a fouling resistance distribution. The results of this analysis are plotted in Fig. 5. The cake fouling resistance was alleviated with the increased ionic strength; however, the pore blocking resistance was stable. The reduction in cake fouling resistance was primarily attributed to the lower HA rejection with the addition of ionic strength, allowing a larger volume of HA pass through the membrane with lower deposition. In terms of the pore blocking resistance, this resistance was mostly owing to the foulant comparable to the pore size of membrane, whereas the ionic strength has little influence on the particle size distribution of HA. Therefore, pore blocking resistances were stable with different ionic strength levels.

3.3. Effect of calcium ions on HA removal, TMP, and fouling resistance distribution

The influence of calcium ions on HA removal and membrane fouling were further studied. As shown in Fig. 6, at the end of the UF process, the HA rejection coefficient was 84.7% with 0.5 mM calcium ion compared to 84.5% for the solution with 2.0 mM. There was a smaller value of 89.07% for the solution with

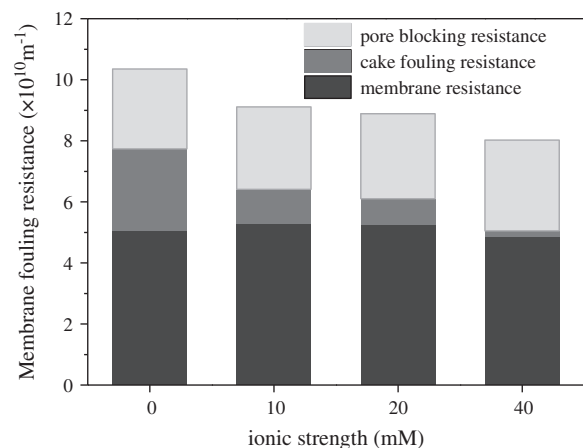


Fig. 5. Effect of different ionic strengths on fouling resistance distribution at the end of UF.

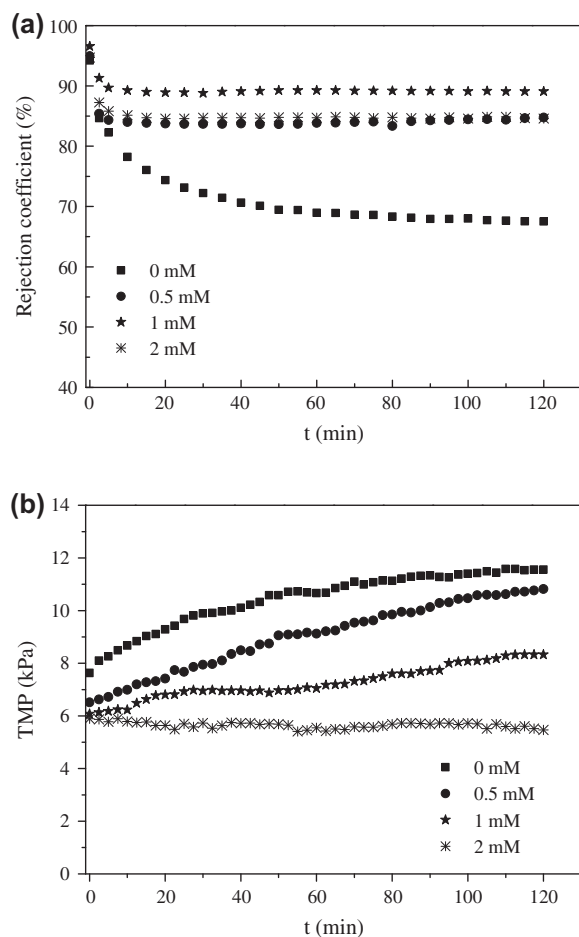


Fig. 6. Effect of different calcium ions on HA removal (a) and TMP (b) development of the UF process.

1.0 mM and much larger value of 67.5% for the solution without extra calcium ions addition. Higher HA rejection rate could be obtained with the addition of calcium ions, which was mainly attributed to the complexation among HA molecules and that between HA molecules and membranes. On the other hand, bridging interactions formed between HA and the membrane led to increase of HA deposition on the membrane, thus increasing the HA rejection coefficient. However, the HA rejection coefficient was lower for 2.0 mM calcium ion than that of 1.0 mM, probably because of the porous structure formed with bigger HA particle size allowed more low MW HA transferred to the effluent.

In addition, it was found in Fig. 6 that the membrane fouling was significantly decreased with the increase of calcium ion concentration from 0 to 2.0 mM. As mentioned in Fig. 2, the size of HA dramatically increase with calcium ions addition. When transported towards the membrane, these

aggregates form a more porous cake layer with relatively high permeability [10], a mitigated TMP was therefore found. This result was in agreement with the result of others [11,12]. However, calcium ions addition was also found to deteriorate the UF behaviors during the treatment of surface water or secondary effluent [3,20,21]. The differences were mostly attributed to the tendentious aggregate interactions, formed between the negative charged functional groups on the membrane surface and the carboxyl groups, or among the carboxyl groups of HA molecules. When complexation happened near the membrane, calcium ions served as bridges, firmly linking foulant molecules to the membrane surface, which resulted in a more serious membrane fouling [22]. In this study, the interaction mostly occurred between carboxyl groups of HA molecules, forming a porous structure. Moreover, there was no membrane fouling with 2.0 mM calcium ions in the UF process, which was likely ascribed to non-resistant cake layer formed with micron scale aggregations, as Lee et al. [23] had shown that particles larger than 1.2 μm would not foul the membrane.

Complexation appears not only on the membrane surface (surface complexation), but also in the bulk solution (bulk complexation). To explain the variation of fouling resistance distribution with different calcium ion concentrations, surface complexation and bulk complexation should be considered simultaneously [23]. Calcium ions mitigated the membrane fouling compared to the base case without calcium ions, and the total membrane fouling resistance decreased with the increase of calcium ion concentration. However, as shown in Fig. 7, fouling resistance distribution showed divergent tendencies with

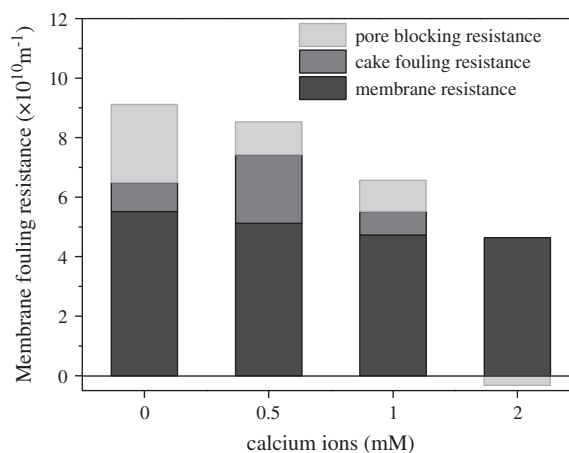


Fig. 7. Effect of different calcium ions on fouling resistance distribution at the end of UF.

relatively lower (0.5 mM) and higher (1.0 and 2.0 mM) calcium ion concentrations. During the UF with low calcium ion concentration (0.5 mM), cake fouling resistance was increased compared to the solution without calcium ions. This phenomenon was likely due to the surface complexation that dominates the interaction with relative low calcium ions. There were two probable evidences for this. Firstly, no significant bulk complexation occurred with calcium ion concentration of 0.5 mM, which was confirmed by the same size distribution of HA molecules between 0 and 0.5 mM calcium ions addition (see in Fig. 2). Secondly, as shown in Fig. 8, the SEM images of the membrane surface indicated that a considerable amount of HA deposited on the membrane surface, which implied that a large amount of surface complexation took place between HA and the negative charged functional groups of the membrane. Calcium ions enhanced the interaction

between HA and the membrane surface, leading to a dense gel layer with high cake fouling resistance. This result was in agreement with Mo et al. [24], who found that a faster gel formation and denser gel layers were formed with calcium ions addition.

Additionally, in the case of higher calcium ion concentrations (1.0 mM and 2.0 mM), both cake fouling resistance and pore blocking resistance were found to be decreased. It was mostly due to the dominated bulk complexation. The bulk complexation was occurred in the solution leading to a much larger HA diameter. There were two changes of fouling resistance. First, the aggregations with high calcium ion concentration were too large to penetrate into the membrane pores, most of them were deposited on the membrane surface, therefore pore blocking resistance was reduced [25]. Second, compared with 0.5 mM calcium ions, the deposited aggregations in 1.0 or

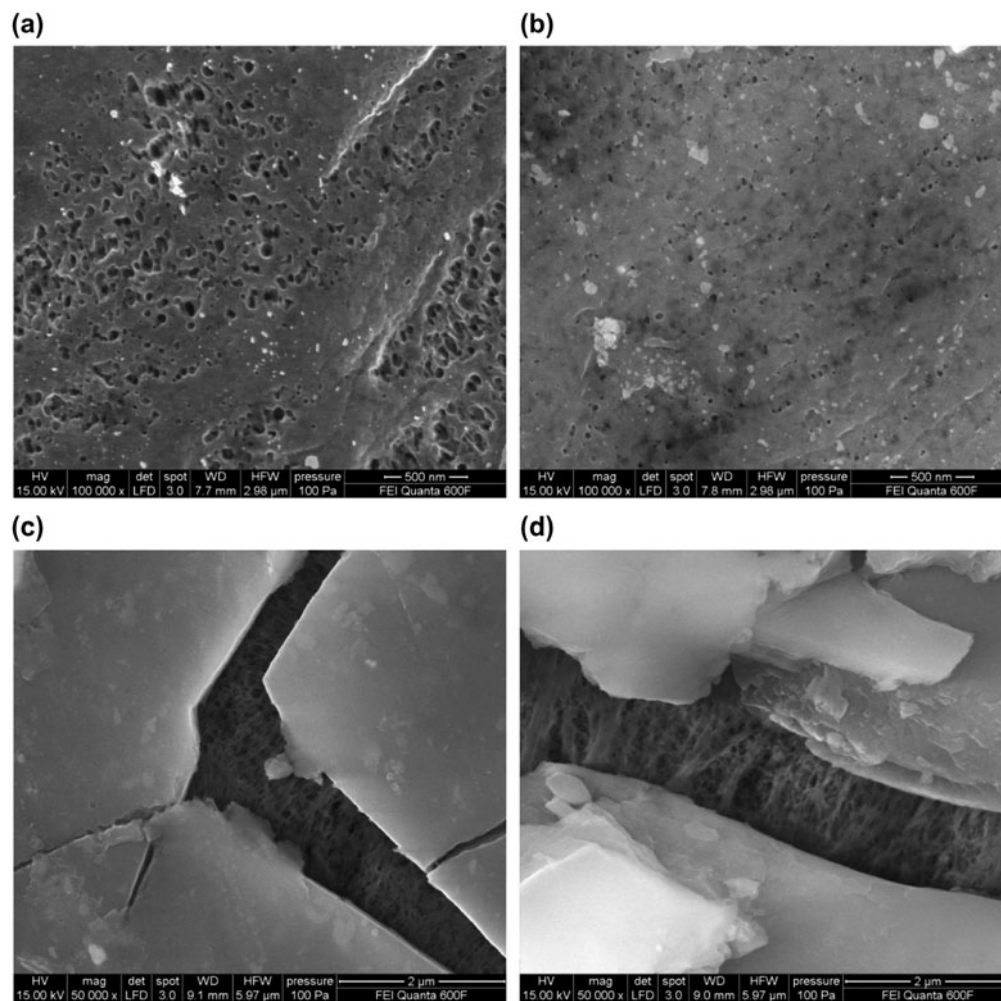


Fig. 8. SEM images of the new membrane and membranes fouled by 20 mg/L HA at different calcium ions concentrations. (a) New membrane, (b) 0 mM, (c) 0.5 mM, and (d) 2.0 mM.

2.0 mM calcium ions was more porous with a lower filtration resistance [26], and the cake fouling resistance was thus alleviated.

3.4. SEM analysis of fouled membrane

SEM images were taken to determine the morphology of the fouling layer on the membrane surface at different calcium ion concentrations. As shown in Fig. 8, there were a great number of large pores present on the new membrane surface. However, as compared with the new membrane, the number of open pores observed on the fouled membrane decreased significantly, and the size of the remaining pores was simultaneously reduced. The phenomenon was owing to pore blocking that restricted the membrane pores and cake layer formation with the deposited HA aggregations that covered the membrane surface. Whereas, no pore could be discovered with calcium ions addition (0.5 or 2.0 mM) for the complexation interaction which leads to a visible cake layer deposited on the membrane surface. It was worth noting that the cake layer formed by 2.0 mM calcium, as shown in Fig. 8, was thicker than that of 0.5 mM although the rejection coefficient was comparable,

which can be explained by the aggregations of larger diameter with 2.0 mM calcium ions addition.

3.5. Schematic model

Based on the results of particle size distribution, HA removal rate, TMP, and fouling resistance distribution in this study, the schematic model of ionic strength and calcium ions on HA fouling is proposed in Fig. 9. HA molecule deposited on the membrane surface and blocked in the membrane pores caused cake fouling and pore blocking. Ionic strength reduced electrostatic repulsive forces between HA molecules and the membrane surface for the decreased zeta potential of HA, which made it easier for HA molecules to penetrate into the effluent, and leading to a lower deposition.

When calcium ions were present in HA solution, aggregation took place between two HA molecules or between HA molecule and membrane surface. In lower calcium ion concentration, the dominated aggregation appeared between HA molecule and membrane surface, and more HA molecules deposited on the membrane surface during the UF, which leads to an increase of cake fouling resistance. In higher calcium ion concentration, the particle of HA changed to a

	System	Deposited HA	Fouling resistance	Schematic model
1	HA	Moderate	Moderate R_p Moderate R_c	
2	HA, ionic strength	Small	Moderate R_p Small R_c	
3	HA, lower calcium	Large	Small R_p Large R_c	
4	HA, higher calcium	Large	Small R_p Small R_c	

HA ionic strength calcium ions membrane negative charge

Fig. 9. Schematic fouling model of HA (1), HA and ionic strength (2), HA and lower calcium (3), and HA and higher calcium (4) on UF.

bigger particle size for the bulk complexation that between two HA molecules. Therefore, cake fouling and pore blocking were mitigated for the particle size changes.

4. Conclusions

Ionic strength and calcium ions were added into HA solution to investigate the influence on HA removal and membrane fouling. The following conclusions could be drawn:

- Both ionic strength and calcium ions addition could effectively reduce zeta potential of the HA solution. Size distribution of HA showed no change with various ionic strength (10, 20, and 40 mM) or lower calcium ions (0.5 mM) concentration, but the particle size of HA increased with higher calcium ions (1.0 and 2.0 mM) concentrations.
- The addition of ionic strength reduced the HA removal significantly, and somewhat mitigated the membrane fouling for a reduction in electrostatic repulsive forces between HA molecules and the membrane surface. The cake fouling resistance was reduced with ionic strength addition.
- In a low calcium ion (0.5 mM) concentration, the surface complexation dominated the fouling behavior of the process, leading to an increase of cake fouling resistance. However, in higher calcium ion concentrations, such as 1.0 and 2.0 mM, the bulk complexation dominated the interaction fouling behavior of the process, which reduced both cake layer fouling resistance and pore blocking resistance.
- A clearly observable thick cake layer formed on the membrane surface with calcium ions addition from SEM analysis.

Acknowledgments

This work was supported by the Major Science and Technology Program for Water Pollution Control and Treatment [grant number 2012ZX07404-003] and the 12th postgraduate sci-tech innovation foundation of Beijing University of Technology [grant number ykj-2013-9605]. We would like to give our sincere thanks to the peer-reviews for their suggestions and discussion.

References

- [1] M. Peter-Varbanets, C. Zurbrügg, C. Swartz, W. Pronk, Decentralized systems for potable water and the potential of membrane technology, *Water Res.* 43(2) (2009) 245–265.
- [2] Y. Hao, A. Moriya, T. Maruyama, Y. Ohmukai, H. Matsuyama, Effect of metal ions on humic acid fouling of hollow fiber ultrafiltration membrane, *J. Membr. Sci.* 376 (2011) 247–253.
- [3] W. Yuan, A. Kocic, A.L. Zydney, Analysis of humic acid fouling during microfiltration using a pore blockage—Cake filtration model, *J. Membr. Sci.* 198 (2002) 51–62.
- [4] Y. Wang, C. Combe, M.M. Clark, The effects of pH and calcium on the diffusion coefficient of humic acid, *J. Membr. Sci.* 183 (2001) 49–60.
- [5] W. Yuan, A.L. Zydney, Humic acid fouling during ultrafiltration, *Environ. Sci. Technol.* 34 (2000) 5043–5050.
- [6] K.L. Jones, C.R. O'Melia, Ultrafiltration of protein and humic substances: Effect of solution chemistry on fouling and flux decline, *J. Membr. Sci.* 193 (2001) 163–173.
- [7] K.S. Katsoufidou, D.C. Sioutopoulos, S.G. Yiantsios, A.J. Karabelas, UF membrane fouling by mixtures of humic acids and sodium alginate: Fouling mechanisms and reversibility, *Desalination* 264 (2010) 220–227.
- [8] A.W. Zularisam, A. Ahmad, M. Sakinah, A.F. Ismail, T. Matsuura, Role of natural organic matter (NOM), colloidal particles, and solution chemistry on ultrafiltration performance, *Sep. Purif. Technol.* 78 (2011) 189–200.
- [9] D. Jermann, W. Pronk, S. Meylan, M. Boller, Interplay of different NOM fouling mechanisms during ultrafiltration for drinking water production, *Water Res.* 41 (2007) 1713–1722.
- [10] J. Shao, J. Hou, H. Song, Comparison of humic acid rejection and flux decline during filtration with negatively charged and uncharged ultrafiltration membranes, *Water Res.* 45 (2011) 473–482.
- [11] F.S. Qu, H. Liang, Z. Wang, H. Wang, H. Yu, G.B. Li, Ultrafiltration membrane fouling by extracellular organic matters (EOM) of *Microcystis aeruginosa* in stationary phase: Influences of interfacial characteristics of foulants and fouling mechanisms, *Water Res.* 46 (2012) 1490–1500.
- [12] J.Y. Tian, M. Ernst, F.Y. Cui, M. Jekel, Effect of different cations on UF membrane fouling by NOM fractions, *Chem. Eng. J.* 223 (2013) 547–555.
- [13] K.H. Choo, C.H. Lee, Membrane fouling mechanisms in the membrane-coupled anaerobic bioreactor, *Water Res.* 30 (1996) 1771–1780.
- [14] W. Yuan, A.L. Zydney, Humic acid fouling during microfiltration, *J. Membr. Sci.* 157 (1999) 1–12.
- [15] C.H. Koo, A.W. Mohammad, F. Suja, M.Z. Meor Talib, Review of the effect of selected physicochemical factors on membrane fouling propensity based on fouling indices, *Desalination* 287 (2012) 167–177.
- [16] J. Lowe, M.M. Hossain, Application of ultrafiltration membranes for removal of humic acid from drinking water, *Desalination* 218 (2008) 343–354.
- [17] X. Wang, K. Chen, J. Qian, X. Li, X. Xiao, Impact of calcium-to-magnesium ratio on the performance of submerged membrane bioreactors, *Desalin. Water Treat.* 49 (2012) 181–188.
- [18] P. van den Brink, A. Zwijnenburg, G. Smith, H. Temmink, M. van Loosdrecht, Effect of free calcium concentration and ionic strength on alginate fouling in cross-flow membrane filtration, *J. Membr. Sci.* 345 (2009) 207–216.

- [19] A. Braghetta, F.A. DiGiano, W.P. Ball, Nanofiltration of natural organic matter: pH and ionic strength effects, *J. Environ. Eng.* 123 (1997) 628–641.
- [20] D.V.W. Van, K.V.T. Sant, I. Pünt, A. Zwijnenburg, A. Kemperman, W.V.D. Meer, M. Wessling, Hollow fiber dead-end ultrafiltration: Influence of ionic environment on filtration of alginates, *J. Membr. Sci.* 308 (2008) 218–229.
- [21] K. Listiarini, W. Chun, D.D. Sun, J.O. Leckie, Fouling mechanism and resistance analyses of systems containing sodium alginate, calcium, alum and their combination in dead-end fouling of nanofiltration membranes, *J. Membr. Sci.* 344 (2009) 244–251.
- [22] W.S. Ang, M. Elimelech, Protein (BSA) fouling of reverse osmosis membranes: Implications for wastewater reclamation, *J. Membr. Sci.* 296 (2007) 83–92.
- [23] C.W. Lee, S.D. Bae, S.W. Han, L.S. Kang, Application of ultrafiltration hybrid membrane processes for reuse of secondary effluent, *Desalination* 202 (2007) 239–246.
- [24] Y. Mo, K. Xiao, Y. Shen, X. Huang, A new perspective on the effect of complexation between calcium and alginate on fouling during nanofiltration, *Sep. Purif. Technol.* 82 (2011) 121–127.
- [25] J. Lohwacharin, K. Oguma, S. Takizawa, Ultrafiltration of natural organic matter and black carbon: Factors influencing aggregation and membrane fouling, *Water Res.* 43 (2009) 3076–3085.
- [26] L.D. Nghiem, D. Vogel, S. Khan, Characterising humic acid fouling of nanofiltration membranes using bisphenol A as a molecular indicator, *Water Res.* 42 (2008) 4049–4058.